Available online at www.sciencedirect.com
SCIENCE DIRECT®
Journal of Nuclear Materials 337–339 (2005) 17–24
journal of nuclear materials
www.elsevier.com/locate/jnucmat

Experimental observations and modelling of carbon transport in the inner divertor of JET

A. Kirschner [a,*], V. Philipps [a], D.P. Coster [b], S.K. Erents [c], H.G. Esser [a], G. Federici [d], A.S. Kukushkin [d], A. Loarte [e], G.F. Matthews [c], J. Roth [b], U. Samm [a], JET EFDA Contributors [1]

[a] *Institut für Plasmaphysik, Forschungszentrum Jülich GmbH, EURATOM Association, Trilateral Euregio Cluster, 52425 Jülich, Germany*
[b] *Max-Planck-Institut für Plasmaphysik, EURATOM Association, Boltzmannstr. 2, 85748 Garching, Germany*
[c] *EURATOM/UKAEA Fusion Association, Culham Science Centre, Abingdon Oxon OX14 3DB, UK*
[d] *ITER JWS Garching Co-center, Boltzmannstr. 2, 85748 Garching, Germany*
[e] *European Fusion Development Agreement, Close Support Unit, 85748 Garching, Germany*

Abstract

In JET, hydrocarbon transport in the inner divertor has been studied on a shot to shot basis by means of a quartz microbalance (QMB) mounted at the entrance of the inner divertor pump duct. Movement of the strike point down the vertical divertor target in the direction of the QMB increases the deposition. Largest carbon deposition is found with the strike point located at the corner of the horizontal divertor plate which offers a direct line-of-sight to the QMB. Monte-Carlo modelling with the ERO transport code reproduces the dependence of material deposition at the QMB on the plasma configuration. A further enhanced carbon flux to the QMB is detected if the strike point is moved for the first time to a location where a carbon layer was built up in former shots. This can be understood in terms of a much larger erosion yield for re-deposited carbon compared with bulk material.

PACS: 52.40.Hf; 52.25.Fi; 52.25.Vy
Keywords: Chemical erosion; Erosion and deposition; ERO-TEXTOR; ITER; Tritium

1. Introduction

In the current design of ITER [1], carbon fibre composites (CFC) are still foreseen for the areas of the divertor target plates nearest the strike point. The main reason for this choice is the requirement to handle off-normal heat loads of more than 10 MW/m^2. Carbon-based materials have the advantage that they do not melt, even under such extreme conditions so that strong material erosion due to melt layer losses will not arise. This benefit is at least partially offset by the main disadvantage of carbon materials which is their erosion due to the formation of hydrocarbon molecules. In contrast to physical sputtering, this chemical erosion process is

* Corresponding author. Tel.: +49 02461 614277; fax: +49 02461 612660.
E-mail address: a.kirschner@fz-juelich.de (A. Kirschner).
[1] See annex of J. Pamela et al., Fusion Energy 2002 (Proc. 19th Int. Conf. Lyon, 2002), IAEA, Vienna.

0022-3115/$ - see front matter © 2004 Elsevier B.V. All rights reserved.
doi:10.1016/j.jnucmat.2004.10.104

effective even at the lowest plasma temperatures. Erosion may lead to a limitation of the lifetime of critical plasma facing components. Of more immediate concern however is the transport of eroded carbon away from the strike zones leading to formation of carbon layers, which retain large amounts of fuel by co-deposition. This co-deposition has been shown to be by far the strongest retention mechanism in present fusion devices. Due to licensing associated with the regulation of safety in nuclear facilities, the maximum amount of retained tritium in ITER must not exceed 350 g. A prerequisite for development of procedures to minimise and remove retained tritium is a detailed knowledge of how carbon is transported, the locations of re-deposition as well as the conditions, which influence the re-deposition and the properties of the re-deposited layers.

In JET and other fusion devices formation of carbon layers has been studied by post-mortem analysis of tiles in between experimental campaigns. Measured deposition patterns represent an average of various plasma conditions and configurations. Since spring 2000 a quartz microbalance (QMB) has been mounted at the entrance of the pump duct in the inner divertor of JET, allowing a shot-resolved measurement of deposition at this special location. This paper presents a brief overview of the current knowledge of carbon transport in JET and then focuses on experimental results obtained with the QMB. The data are compared with Monte-Carlo modelling of carbon transport for the inner divertor.

2. Carbon transport and deposition in JET

2.1. Overview of past results

Analysis of divertor tiles from JET MkIIA after divertor plasma operation of about 18 hrs has shown that the inner divertor is everywhere deposition dominated with most of the deposition on the water cooled louvers at the entrance of the pump duct [2]. Only very little deposition is seen in the outer divertor including the louver region. This behaviour is not fully understood but flows in the scrape-off-layer (SOL), which are directed to the inner divertor [3] and drive carbon eroded at the main chamber to the inner divertor are thought to play an important role. Asymmetries in plasma parameters between the two divertor legs leading to differences in the local balances between erosion and deposition processes may also be important. The total amount of carbon deposited on the inner louvers is estimated to be about 900 g corresponding to a carbon deposition rate of 7×10^{20} C/s, which is 1% of the total deuterium ion flux arriving at the inner divertor. If standard assumptions for chemical erosion (1–2%) and for sticking of re-deposited carbon species (according to TRIM database or molecular dynamic calculations) are applied, the ERO Monte-Carlo code prediction for the carbon deposition at the inner louver region of the MkIIA divertor is much smaller than the measured carbon deposition [5]. Much closer agreement with experiment was obtained when the sticking probability of returning hydrocarbon fragments was arbitrarily set to zero and a plasma configuration with the strike point near to the louver entrance was utilised. In our picture, zero sticking is understood in terms of a very high probability for the re-deposited hydrocarbons to be re-eroded at plasma-wetted areas. A very similar picture has been deduced from dedicated experiments in TEXTOR where $^{13}CH_4$ was injected through test limiters and their deposition was compared with ERO modelling [6].

After the JET MkIIGB gas box divertor operation (1999–2001) tile analysis again revealed a net-deposition zone in the inner divertor with a layer thickness of up to about 80 μm [7]. As with MkIIA, over most of the outer divertor area in MkIIGB erosion is balanced by deposition while only a small zone close to the entrance of the pump ducts on the horizontal target is deposition dominated [8]. Again, asymmetric flows and plasma conditions drive the eroded carbon mainly to the inner divertor leading to strong deposition on the tiles, in particular on the shadowed parts of the inner horizontal tiles. The total amount of carbon deposition on plasma facing sides and shadowed areas of the horizontal tiles is estimated to about 400 g during a total plasma divertor time of 16 hrs. The overall carbon deposition rate is thus 5×10^{20} C/s, slightly lower compared with MkIIA operation. However, in MkIIA the majority of carbon deposition in the inner divertor is at the remote louvers (~90%) while in MkIIGB the majority is deposited on the divertor tiles themselves, mainly on the shadowed part of the horizontal tiles.

2.2. Measurement of carbon deposition on the louver area using a quartz microbalance

A specially designed quartz microbalance (QMB) has been mounted at the entrance of the inner louver region of JET during the recent MkIIGB-SR divertor operation campaign for which the septum has been removed. The measurement is based on the change of the resonance frequency of a quartz crystal caused by the change of its mass due to material deposition or erosion. The QMB system allows shot-by-shot measurements of deposition with a resolution of about 0.4 nm. Details of the QMB system in JET are described in [9].

The QMB, which is equipped with a shutter, has been exposed from march 2002 until the end of 2003 to about 600 discharges corresponding to a total exposure time of 4900 s. The material deposition averaged over about 310 shots with various plasma configurations, heating power, L- and H-mode is about 1.5×10^{19} C/s [10,11].

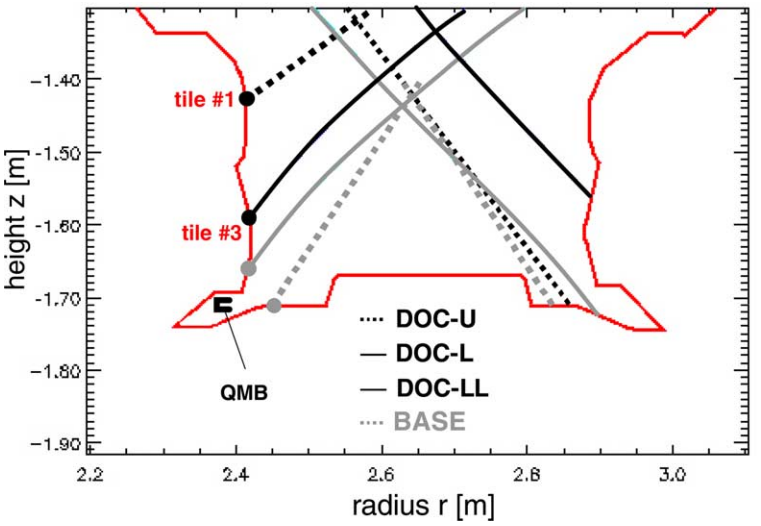

Fig. 1. Diagnostic optimised configurations (DOC) of the divertor plasma in JET.

This averaged value shows a much smaller mean carbon transport towards the inner louver area compared with the MkIIA operation, estimated to about 7×10^{20} C/s. However, the most striking result is that the material deposited on the QMB depends strongly on the geometry of the plasma configuration in the divertor. Fig. 1 shows a schematic view of the different DOC configurations (Diagnostic Optimised Configurations to optimise the edge diagnostics) and in addition a configuration with the strike point located on the horizontal plate (BASE case). In the DOC-U configuration the inner strike point is located on the upper part of the vertical plates, moved down on the lower part of the vertical plates in DOC-L and positioned on the lower end of the vertical plates in DOC-LL. The QMB data show an increased deposition if the strike point is moved down the vertical targets towards the QMB. For H-mode discharges, above an input power of 8 MW, the averaged deposition is mostly below the detection limit of about 5×10^{14} C/cm^{2}s in DOC-U plasmas. In the DOC-L configuration where the strike point moved by about 20 cm downwards the deposition increases to about 1.4×10^{15} C/cm^{2}s on average and increases yet again for the even lower DOC-LL configuration (factor of about 1.5). Moving the strike point to the horizontal plate (BASE configuration) increases the deposition even more, on average by a factor of about 6 compared to DOC-LL cases.

The QMB data also show that the carbon deposition and thus the erosion source can be significantly stronger if the plasma configuration is changed such that surfaces are touched for the first time by plasma impact. This enhanced carbon transport reduces in subsequent discharges suggesting once more an enhanced erosion of re-deposited carbon layers, which has been found in beam experiments [12]. Fig. 2 shows an example of this effect on a series of similar H-mode discharges. Changing from DOC-L to DOC-LL configuration the deposition increases by a factor of about 9. Going back to DOC-L leads to no deposition (rather erosion). The deposition is about a factor of three smaller for the strike point moved back to the horizontal plate compared with the former shot where the strike point was moved for the first time to this position. This indicates that a layer is deposited on the horizontal target near the entrance of the louver region during previous plasma operation, which is then preferentially eroded during the horizontal plate plasma operation. Similar observations are obtained from locally resolved carbon spectroscopy in the inner divertor [13]. More detailed QMB results are described in [11].

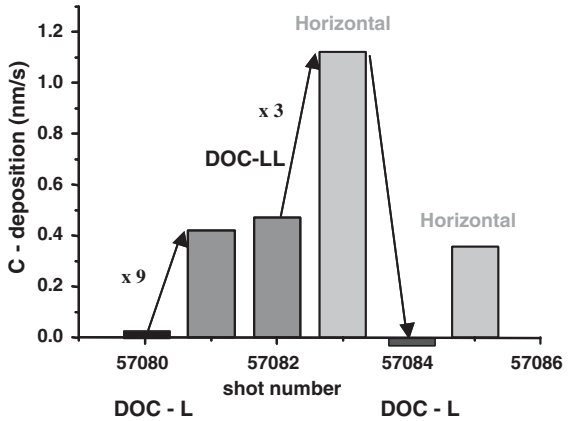

Fig. 2. Deposition on QMB for subsequent H-mode discharges with different plasma configurations.

2.3. Modelling of carbon deposition on the QMB monitor

Transport of carbon in the inner divertor of JET MkIIGB-SR has been modelled with a variant of the three-dimensional Monte-Carlo Code ERO [4]. Neutrals, which are physically or chemically eroded according to semi-empirical models (such as the Bohdanski/Yamamura [14,15] formula for physical sputtering or the Roth formula [16] for chemical erosion) leave the solid with a Maxwell or Thompson velocity and cosine angular distribution. They become ionised or dissociated following rate coefficients (such as the Lotz [17] formula for atomic species or Janev/Reiter [18] database for hydrocarbons) depending on the local plasma parameters. Movement of charged particles is governed by Lorentz-forces, friction with the background plasma, thermal forces and diffusion. These forces lead to a certain re-deposition of eroded particles on the surface. The transport calculation for a single test particle is terminated if the particle is re-deposited or has left the simulation volume.

As input for the ERO calculations the two-dimensional distribution of the plasma parameters inside a poloidal cross section are calculated with the B2-Eirene [19,20] package. Three different plasma configurations are used: DOC-U, DOC-L and a configuration with the inner strike point located on the horizontal target (BASE configuration). For all three cases an input power of 12 MW with a radiation fraction of 30% is used. The B2-Eirene solutions correspond to steady-state modelling representing plasma conditions time-averaged over many ELM periods. Thus surface heating effects caused by an increased power flux during ELMs are not taken into account. Fig. 3 shows the resulting profiles of ion flux along the inner target plates. A more detailed discussion of the plasma parameters for the DOC-U and DOC-L cases is given in [21].

2.3.1. Carbon transport in DOC-L configuration

For the ERO modelling, the simulation volume in z-direction towards the main plasma ends at $z = -1.5$ m, in radial direction the volume ends at $r = 2.6$ m. The other boundaries are given by the tile geometry. The transport of chemically eroded CD_4 and physically sputtered carbon atoms is treated separately. To elucidate a possible effect of low sticking for hydrocarbon radicals or respectively of high re-erosion probability [6], sticking S of hydrocarbon species returning to the divertor plates is varied between 0 and 1.

2.3.1.1. Chemical erosion: assumption of sticking one for hydrocarbon radicals and carbon atoms. First, a chemical erosion yield of 1% has been assumed with erosion only due to deuterium ions. Changes of the erosion yield and erosion by deuterium atoms will be addressed later. For chemical erosion formation of CD_4 molecules is assumed. Dissociation and ionisation rates for CD_y species are taken from [18].

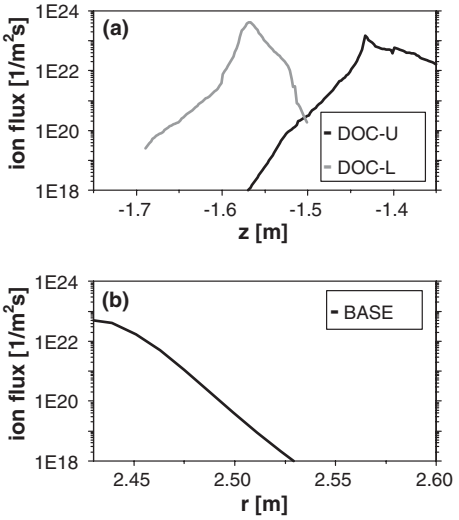

Fig. 3. Ion flux profiles along the inner divertor plates of JET MkIIGB-SR modelled with B2-Eirene for three different plasma configurations (input power of 12 MW and 4 MW radiation).

Fig. 4(a) shows the gross-erosion and re-deposition along the divertor tiles for a sticking coefficient of unity for all returning species. The x co-ordinate (distance s along the plates) starts on the vertical tile #1 at $z = -1.45$ m, reaches $s = 350$ mm at the lower end of the vertical tile #3 and reaches values larger than $s = 350$ mm on the horizontal tiles (see Fig. 1). As can be seen nearly all eroded particles are re-deposited near their starting location resulting from very small penetration into the plasma (especially near the strike point). The integrated amount of re-deposition on the divertor tiles is about 99%. Fig. 4(b) shows the difference of re-

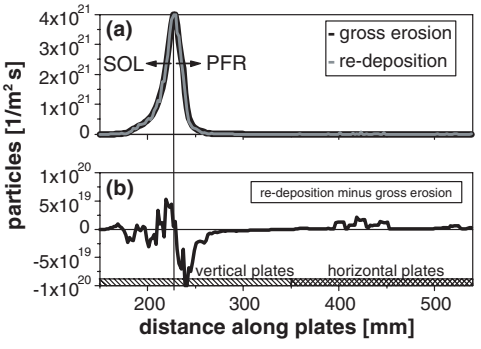

Fig. 4. Simulated profiles along the inner divertor plates of gross-erosion and re-deposition (a) and net-deposition (b) for chemical erosion in DOC-L. Sticking of hydrocarbons and atoms is assumed to be one.

deposition and gross-erosion. A zone (width ~20 mm) of net-deposition occurs near the strike point inside the scrape-off-layer (SOL) and a net-erosion zone downwards the target to the direction of the private flux region (PFR). The net-deposition zone results from particles eroded in the SOL and then re-deposited at the target shifted to the direction of the PFR (towards higher *s*-values) due to the penetration into the near surface plasma, ionisation and transport along the magnetic field lines. Particles, which are eroded below the strike zone at the beginning of the PFR have a much higher probability to reach the low density PFR plasma and therefore are more likely to escape in the direction of the horizontal plates or towards the outer divertor (visible as net-erosion in Fig. 4(b)). The amount of particles leaving through the gap of the louver region is only about 0.02% of the eroded species yielding an absolute number of about 5.5×10^{13} C/cm^{2}s. It should be remembered that only a certain fraction of particles entering the louver region is finally deposited on the louver itself. Detailed modelling of the particle transport in the louver region predicts this fraction to be about 50% [22], for which the simulated values have to be divided by two to get a deposition rate. The modelled deposition rate is therefore about a factor of 50 smaller than that measured by the QMB.

2.3.1.2. Chemical erosion: assumption of zero sticking for hydrocarbon radicals and molecular dynamic reflection for carbon atoms. If we assume the other extreme case of zero sticking coefficient for all returning hydrocarbons and reflection coefficients for carbon atoms according to molecular dynamic calculations [23], ERO predicts the gross-erosion, re-deposition and net-deposition profiles shown in Fig. 5. A broader zone of erosion appears around the strike point with no clear net-deposition on the whole vertical target: this results from the fact that only carbon atoms can be re-deposited whereas all hydrocarbons are re-injected into the plasma leading to a higher particle loss rate into the PFR. The integrated re-deposition on the divertor plates decreases from 99% (for $S = 1$) to about 84%. About 10% of the eroded particles leave the simulation volume into the direction of the outer divertor. Most of the remaining fraction leaves towards the main plasma. Compared with sticking one, the amount of particles transported into the louver region increases by a factor of about 7 to 0.14% or 3.8×10^{14} C/cm^{2}s. However, compared to findings from QMB measurements this value is still about a factor of 7 to small.

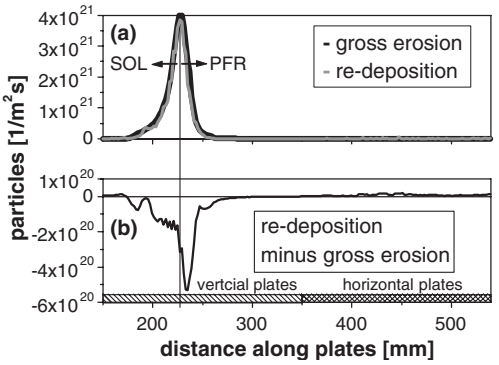

Fig. 5. Simulated profiles along the inner divertor plates of gross-erosion and re-deposition (a) and net-deposition (b) for chemical erosion in DOC-L. Sticking of hydrocarbons is assumed to be zero, sticking of carbon atoms according to molecular dynamics calculations.

2.3.1.3. Chemical erosion: influence of the erosion yield. As mentioned, a chemical erosion yield of 1% for deuterium ions has been assumed so far and erosion by atoms has been neglected. Compared to QMB measurements, the modelling predicts a carbon deposition on the louver in the DOC-L configuration which is seven times too small, even for the extreme assumption of zero sticking for returning hydrocarbons. For fully sticking this discrepancy increases to a factor of 50. The new empirical fitting formula, which has been developed to describe the chemical erosion yield in dependence on flux, impact energy and surface temperature [24] results in a very similar yield of about 1% near the strike point assuming a surface temperature of about 900 K where the chemical erosion has its maximum. Typically, this temperature is not reached all along the target in JET. However, at the lower flux densities found away from the strike points, the Roth formula predicts larger erosion yields.

In any case, the inner divertor is a deposition dominated region where carbon eroded from the main chamber is deposited and subsequently re-eroded. These deposited carbon layers can suffer from an enhanced chemical erosion yield. Indeed, chemical erosion yields of up to 10% have been deduced from spectroscopy in the inner divertor of JET [25]. In addition, erosion by deuterium atoms can be assumed to contribute to the overall chemical erosion [26]. These effects increase the simulated amount of carbon entering the louver region by a significant factor (5–10). A more precise modelling would need better validated chemical erosion yields in the inner divertor of JET (which is difficult because the plasma usually detaches when hydrocarbons are injected). It should also be mentioned again that a possible effect of ELMs is not included in the present simulations. Nevertheless it can be concluded, that a satisfactory agreement between simulation and experiment is achieved assuming a low effective sticking of hydrocarbons ($S \sim 0$ to be interpreted as high 'self re-erosion' of deposited layers) and an erosion yield as suggested by the Roth formula for impinging background deuterium ions and atoms.

2.3.1.4. Physical sputtering: assumption of molecular dynamic reflection for carbon atoms. Fig. 6 shows simulated profiles of gross-erosion, re-deposition and net-deposition for physically sputtered carbon. About 73% of the eroded C atoms are re-deposited on the plates. The remaining amount of particles leave the simulation volume in the z-direction (19%) and towards the outer divertor region (8%). For the DOC-L configuration, no physically eroded carbon can enter the louver region. The physically eroded particles originate from a region almost fully located in the SOL, whereas physical sputtering becomes zero due to low plasma temperatures at s values larger than 240 mm (Fig. 6(a)). Particles not locally re-deposited on the vertical target are transferred through the low density PFR in the direction of the outer divertor region or to the horizontal plate of the inner divertor. Due to their starting location of s smaller than 240 mm, physically eroded particles impinge on the horizontal plate at s values larger than 440 mm. Reflection from these locations into the louver region is extremely unlikely. In comparison, part of the chemically eroded particle flux hits the horizontal plate already at values of s larger than 360 mm (see Fig. 4(b)), which increases the probability of reflection into the louver region. A net-erosion zone near the maximum of gross-erosion appears (Fig. 6(b)) followed again by a net-deposition area. The pronounced development of the net-deposition maximum results from the fact that the gross-erosion peak is located deeper in the SOL, in contrast to the situation for chemical erosion.

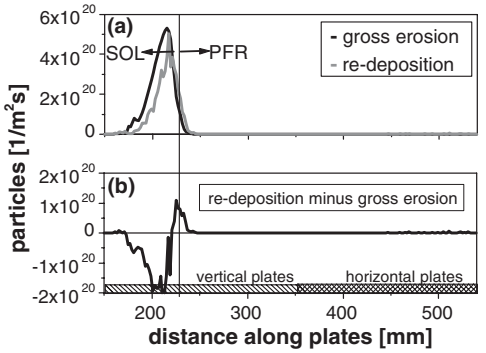

Fig. 6. Simulated profiles along the inner divertor plates of gross-erosion and re-deposition (a) and net-deposition (b) for physical sputtering in DOC-L. Sticking of carbon atoms is assumed according to molecular dynamics calculations.

2.3.2. Dependence of carbon transport on strike point position

More important than absolute values is the comparison of the three different plasma configurations which is summarised in Table 1 for chemical erosion and physical sputtering. This table also shows mean deposition rates from QMB measurements for H-Mode shots with an input power larger than 8 MW.

In DOC-U configuration the amount of chemically eroded carbon entering the louver region is very small. Compared to DOC-L the relative amount (related to the number of eroded particles) decreases by a factor of 50 for fully and about 16 for zero sticking. The corresponding absolute values decrease by a factor of 100 for $S = 1$ and 30 for $S = 0$ (the gross-erosion in DOC-U is about a factor of two smaller than in DOC-L). This is in agreement with QMB measurements which show a decrease of at least a factor of three changing from DOC-L to DOC-U (the measured values for DOC-U are below the detection limit). Similarly to the DOC-L configuration, transport of physically eroded particles to the louver region is negligible in DOC-U. In the BASE configuration with the strike point on the horizontal target, the modelled relative amount of chemically eroded particles reaching the louver region increases by a factor of about 150 compared with DOC-L and the absolute number by a factor of about 60. No significant difference in these factors occurs between the assumptions $S = 1$ and $S = 0$ for hydrocarbons. The main reason for this large increase is that the BASE configuration offers a direct line-of-sight for eroded and reflected particles to the louver region. This behaviour is in clear agreement with QMB observations, which show highest deposition with the strike point on the horizontal plate although the increase changing from DOC-L to BASE is less pronounced. In contrast to

Table 1
Simulated amount of particles entering the inner louver region in dependence on the plasma configuration and sticking assumptions together with average deposition rates from QMB measurements for discharges with input power larger than 8 MW

Plasma configuration	Chemical erosion (1%) $S = 1$		Chemical erosion (1%) $S = 0$		Physical erosion		QMB
	$\frac{\#\text{louver}}{\#\text{erosion}}$ [%]	Louver [C/cm^2 s]	$\frac{\#\text{louver}}{\#\text{erosion}}$ [%]	Louver [C/cm^2 s]	$\frac{\#\text{louver}}{\#\text{erosion}}$ [%]	Louver [C/cm^2 s]	Deposition [C/cm^2 s]
DOC-U	4×10^{-4}	5.5×10^{11}	9×10^{-3}	1.3×10^{13}	0.0	0.0	$< 5.0 \times 10^{14}$
DOC-L	0.02	5.5×10^{13}	0.14	3.8×10^{14}	0.0	0.0	1.4×10^{15}
BASE	3.7	4.0×10^{15}	21.8	2.3×10^{16}	12.5	8.3×10^{15}	1.2×10^{16}

According to [22] about 50% of particles entering the louver region are deposited on the louver wherefore the simulated values have to be divided by two to obtain deposition rates on this area.

DOC-U and DOC-L configurations, physically eroded particles can be transported to the louver region in BASE configuration.

Deposition on the QMB in BASE configurations shows also a dependence on the history of previous discharges (Section 2.2). The simulations show that in configurations with the strike point on the vertical target part of the eroded carbon is deposited on the horizontal plate. These deposition zones are shifted nearer to the louver and the amount of re-deposition increases if the strike point is located further down the vertical target. In such configurations carbon is not re-deposited locally and is partly re-deposited on the base plate from where it can be re-eroded during a base plate discharge (with an enhanced erosion yield) and transported towards the louver. Such behaviour is indeed seen experimentally. This shows that part of the carbon transport is stepwise from one location to another driven by different (geometrical) plasma configurations. Such behaviour is also in line with carbon transport studies using $^{13}CH_4$ methane injection from top of JET in dedicated discharges in a given plasma configuration (DOC-L like) at the end of a campaign, followed by surface analysis for ^{13}C deposition. In this experiment, most of the ^{13}C was found on the inner vertical tiles with no measurable amount on the shadowed region of the horizontal tile at the entrance to inner louver region [27].

3. Conclusions

New shot-resolved deposition measurements by means of a quartz microbalance at the entrance of the inner divertor louver region in JET (MkIIGB-SR divertor) show that the carbon transport to this remote region depends on the geometrical position of the strike point. With the strike point on the upper vertical target (DOC-U) the deposition is below the detection limit and increases with the strike point moving down. Largest deposition occurs if the strike point is located at the lower end of the vertical plates (DOC-LL configuration) or on the horizontal target. This dependence is very well in line with ERO modelling of carbon transport towards the QMB location. Modelled absolute deposition rates for a standard 12 MW H-mode discharge agree within a factor of 2–4 with the experimental data assuming enhanced erosion of re-deposits (in the modelling negligible sticking of hydrocarbons, $S \sim 0$). The simulations show that plasma configurations with the strike point at the lower end of the vertical target (DOC-LL like) lead preferentially to deposition on the horizontal plate which can be re-eroded effectively with the plasma positioned on this plate. Such behaviour is indeed observed experimentally showing an enhanced deposition on the QMB depending on the history of previous discharges. Carbon transport towards special locations therefore can occur stepwise involving different plasma configurations. Deposition patterns from post-mortem tile analysis thus represent the average of many different plasma geometries during the corresponding operation campaign.

In order to model absolute deposition on the louver, small effective sticking or enhanced re-erosion of freshly re-deposited carbon must be assumed. This is in agreement with modelling of transport of injected $^{13}CH_4$ in TEXTOR and of carbon transport in JET MkIIA. Implications for ITER are discussed in detail in [24].

Acknowledgments

This work is being carried out under the research programme activities of the European Task Force of Plasma-Wall-Interactions and partially funded by task TW3-TPP-ERMOD of the EFDA technology programme. It is partly funded by EURATOM and in the UK by United Kingdom Engineering and Physical Sciences Research Council.

References

[1] ITER Technical Basis, ITER EDA Documentation Series No. 24, IAEA, Vienna, 2002.
[2] J.P. Coad et al., J. Nucl. Mater. 290–293 (2001) 224.
[3] S.K. Erents et al., Proceedings of the 26th EPS Conference on Controlled Fusion and Plasma Physics, Maastricht, June 1999.
[4] A. Kirschner, V. Philipps, J. Winter, U. Kögler, Nucl. Fusion 40 (5) (2000) 989.
[5] A. Kirschner et al., Plasma Phys. Control. Fusion 45 (2003) 309.
[6] A. Kirschner et al., J. Nucl. Mater. 328 (2004) 62.
[7] J.P. Coad et al., J. Nucl. Mater. 313–316 (2003) 419.
[8] M. Mayer et al., Phys. Scr. T 111 (2004) 55.
[9] H.G. Esser et al., Fusion Eng. Des. 66–68 (2003) 855.
[10] H.G. Esser et al., Phys. Scr. T 111 (2004) 129.
[11] H.G. Esser et al., these Proceedings. doi:10.1016/j.jnucmat.2004.10.112.
[12] E. Vietzke, K. Flaskamp, V. Philipps, et al., J. Nucl. Mater. 145–147 (1987) 443.
[13] S. Brezinsek et al., these Proceedings. doi:10.1016/j.jnucmat.2004.10.114.
[14] W. Eckstein, C. Garcia-Rosales, J. Roth, W. Ottenberger, Sputtering Data, Report IPP9/82, Max-Planck-Institut für Plasmaphysik, Garching, 1993.
[15] Y. Yamamura, Y. Itikawa, N. Itoh, Report IPP JAM-26, NIFS, Nagoya, 1983.
[16] J. Roth, J. Nucl. Mater. 266–269 (1999) 51.
[17] W. Lotz, Z. Phys. 220 (1969) 466.
[18] R.K. Janev, D. Reiter, Jülich Report, Jül-3966, 2002.
[19] B.J. Brahms, Computational studies in tokamak equilibrium and transport, PhD thesis, Rijksuniversiteit, Utrecht, Netherlands, 1986.
[20] D. Reiter, J. Nucl. Mater. 196–198 (1992) 80.

[21] D.P. Coster et al., J. Nucl. Mater. 313–316 (2003) 868.
[22] J.N. Brooks, A. Kirschner, D.G. Whyte, et al., J. Nucl. Mater. 313–316 (2003) 424.
[23] D.A. Alman, D.N. Ruzic, Phys. Scr. T 111 (2004) 145.
[24] J. Roth et al., these Proceedings. doi:10.1016/j.jnucmat.2004.10.115.
[25] M.F. Stamp et al., J. Nucl. Mater. 290–293 (2001) 321.
[26] G. Federici et al., J. Nucl. Mater. 313–316 (2003) 11.
[27] J. Likonen et al., Fusion Eng. Des. 66–68 (2003) 219.